Isabelle M. Palstra, Hugo M. Doeleman, and A. Femius Koenderink

Supplementary Material for "Hybrid cavity-antenna systems for quantum optics outside the cryostat?"

1 Comparison between ellipsoid dimers and bow-tie antennas

Here we show a comparison between the quality factors and LDOS enhancements (parametrized through antenna mode volumes) of ellipsoid antennas and bow-tie antennas. As mentioned in the main text, bow-tie antennas form a good alternative to ellipsoid dimers, as these can be lithographically fabricated (albeit not with gaps below ~ 5 nm) [1]. Here we argue that the results discussed in the main paper for ellipsoid dimers hold equally well for bow-tie antennas with similar gaps, since these can achieve similar figures of merit.

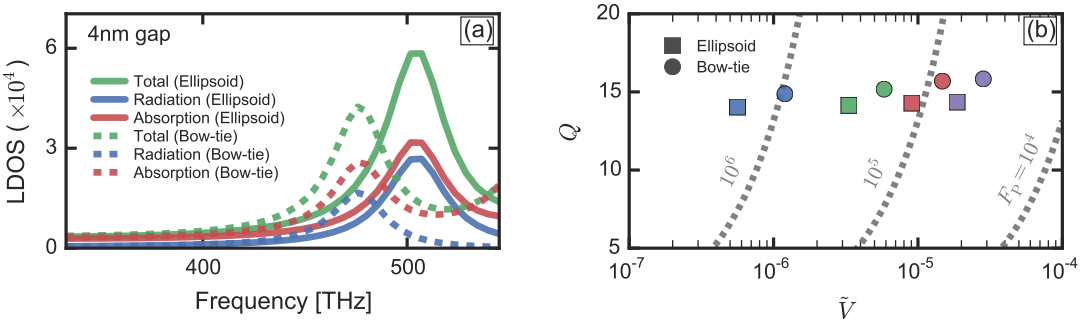

Fig. 1: Comparison of LDOS spectra, Q and $\tilde{V}$ between ellipsoid dimers and bow-tie antennas. (a) LDOS spectra of an ellipsoid dimer and a bow-tie antenna, both with a gap of 4 nm. We see similar linewidths and peak heights, even if exact resonance frequencies are different. **(b)** Comparison of Q and $\tilde{V}$ for ellipsoid dimers and bow-tie antennas with gaps of 1 (blue), 2 (green), 3 (red) and 4 nm (purple). We see the same scaling with gap size for both antennas. Quality factors are strongly alike and mode volumes differ by up to a factor ~ 2. For all simulations, the point source was oriented along the antenna long axis and situated in the center of the antenna gap.

To verify the similarity between bow-ties and ellipsoid dimers, we perform finite element simulations of both. Ellipsoid dimer simulations are described in the main text, and here we consider only the antennas with an ellipsoid length of 80 nm and gaps of 1-4nm. We design bow-tie antennas consisting of two equilateral triangles of 40 nm height and 70 nm side length, with the tips facing each other and seperated by gaps of 1-4 nm. All edges and points are rounded with rounding radius of 2.5 nm, preventing unphysical hot-spots due to sharp edges. A point source is placed at the center of the bow-tie gap, oriented along the antenna long axis.

Figure 1a shows a comparison between the LDOS spectra of an ellipsoid dimer and a bow-tie with gaps of 4 nm. Resonance frequencies and albedo (ratio of scattering to total LDOS) are different, but these can be tuned through, e.g., height and size. The important point is that both achieve similar linewidths and peak

Isabelle M. Palstra, Hugo M. Doeleman, These authors contributed equally
A. Femius Koenderink, Corresponding author: f.koenderink@amolf.nl
Isabelle M. Palstra, Hugo M. Doeleman, A. Femius Koenderink, Center for Nanophotonics, AMOLF, Science Park 104, 1098 XG Amsterdam, The Netherlands, and Van der Waals-Zeeman Institute, Institute of Physics, University of Amsterdam, Science Park 904, PO Box 94485, 1090 GL Amsterdam, The Netherlands.

LDOS, which is what matters most for the hybrid performance. Figure 1b shows Q and $\tilde{V}$ for ellipsoids and bow-ties with gap sizes between 1 and 4 nm. Again, Q is almost identical and, although there are differences in the exact mode volumes due to the difference in peak LDOS, ellipsoid and bow-tie mode $\tilde{V}$ have the same order of magnitude and show the same scaling with gap size. These results show that hybrids composed of bow-tie antennas coupled to cavities should achieve similar figures of merit as demonstrated in the main paper for ellipsoid dimers.

2 A coupled oscillator model for hybrid cavity-antenna systems

Here we briefly describe the coupled oscillator model used to predict LDOS in a hybrid cavity-antenna system. For a more detailed description, we refer to an earlier work [2]. The coupled equations of motion describing a coupled antenna-cavity system, driven by a point dipole (i.e., classical representation of a quantum emitter) p_{dr} at frequency ω are

$$\left(\omega_{\mathrm{a}}^2 - \omega^2 - i\omega\gamma_{\mathrm{a}}\right) p - \beta E_{\mathrm{c}} = \beta G_{\mathrm{bg}} p_{\mathrm{dr}}, \tag{1}$$

$$\left(\omega_{\mathrm{c}}^2 - \omega^2 - i\omega\kappa\right) E_{\mathrm{c}} - \frac{\omega^2}{\epsilon_0 \epsilon V_{\mathrm{c}}} p = \frac{\omega^2}{\epsilon_0 \epsilon V_{\mathrm{c}}} p_{\mathrm{dr}}. \tag{2}$$

where the induced antenna dipole moment p and the excitation of the cavity mode field E_{c} are the free variables, ω_{a} (ω_{c}) and γ_{a} (κ) describes antenna (cavity) resonance frequency and damping rate, respectively, β is antenna oscillator strength (for example, $\beta = 3V_{\mathrm{ant}}\epsilon_0\omega_{\mathrm{a}}^2$ for a Drude-metal sphere of volume V_{ant}), G_{bg} is the background Green's function determining antenna-source coupling strength, V_{c} is cavity mode volume and $\epsilon = \epsilon(\vec{r}_{\mathrm{a}})$ is the relative permittivity at the antenna location. Importantly, $\gamma_{\mathrm{a}} = \gamma_{\mathrm{i}} + \gamma_{\mathrm{r}}$ includes both Ohmic damping γ_{i} and radiative damping γ_{r}, ensuring that the model is self-consistent and applicable both to strongly and weakly scattering antennas [3]. To find LDOS, we calculate the power emitted by the source dipole, given as [4]

$$P_{\mathrm{dr}} = \frac{\omega}{2} \operatorname{Im}\left\{p_{\mathrm{dr}}^* E_{\mathrm{tot}}\right\}, \tag{3}$$

where E_{tot} is the total field at the source position, which can be found by solving the equations of motion Eqs. (1) and (2) and which consists of several multiple-scattering contributions. Normalizing P_{dr} to the power emitted by the source in vacuum yields the total LDOS, given by Eq. (3) in the main text.

3 Predicting hybrid performance using a coupled oscillator model

Here we explain how we predict hybrid LDOS, Q and $\tilde{V}$ using a coupled oscillator model and parameters retrieved from finite-element simulations of the bare cavity and antenna. The LDOS in a hybrid system is given by Eq. (3) in the main text. To evaluate this equation, for example to produce spectra as in Fig. 4a of the main text, we need the following information: cavity resonance frequency ω_{c}, linewidth κ and effective mode volume V_{c}, as well as antenna polarizability α and the background Green's function G_{bg} determining antenna-source coupling strength. Note that, while Eq. (1) explicitly assumes a Lorentzian response for the bare antenna, this is not a necessary condition for Eq. (3) in the main text to hold. If α can be retrieved directly, knowledge of ω_{a}, γ_{a} and β individually (which determine α for a Lorentzian dipole antenna) is not required.

Cavity parameters are obtained from a finite-element simulation of the cavity, driven by point dipole 25 nm above the top surface at the center of the nanobeam, oriented in the y-direction (in the frame of Fig. 2a in the main text). We calculate emitted power and normalize to the power emitted in vacuum to obtain the LDOS spectrum shown in Fig. 2c of the main text. The coupled oscillator predicts a bare cavity LDOS spectrum given as [2]

$$\mathrm{LDOS}_{\mathrm{c}} = 1 + \frac{6\pi\varepsilon_0 c^3}{\omega^3 n} \operatorname{Im}\left\{\chi_{\mathrm{c}}\right\}, \tag{4}$$

that is, just the last term in Eq. (3) in the main text, with hybridized cavity response χ_{H} replaced by the bare cavity Lorentzian response function

$$\chi_{\mathrm{c}} = \frac{1}{\epsilon_0 \epsilon V_{\mathrm{c}}} \frac{\omega^2}{\omega_{\mathrm{c}}^2 - \omega^2 - i\omega\kappa}. \tag{5}$$

Equation (4) is fitted to the simulated LDOS spectrum (see Fig. 2c of the main paper) to obtain ω_{c}, κ and V_{c}.

To get antenna parameters, finite element simulations of a bare antenna could be combined with a similar fit as for the cavity, as was also done in earlier work [2]. Here, however, we choose not to use a fit but instead a direct retrieval method. This largely circumvents problems due to non-dipolar contributions to the antenna LDOS, such as non-resonant quenching at very small gaps or multipolar resonances at high frequencies. Polarizability α is thus directly calculated by integrating polarization currents in an antenna driven by an external plane-wave, polarized along the antenna long axis. We then perform another simulation of the same antenna, now driven by an x-oriented point dipole at the center of the dimer gap (in the frame of Fig. 2d in the main text), producing LDOS spectra as shown in Fig. 2h of the main text. The coupled oscillator predicts a bare antenna radiative LDOS spectrum given as [2]

$$\mathrm{LDOS}_{\mathrm{r,a}} = \left|1 + \alpha G_{\mathrm{bg}}\right|^2. \tag{6}$$

If we assume that G_{bg} is real and positive (i.e. no phase delay between the source dipole moment and the field driving the antenna), which is a good approximation for a source positioned in the hotspot of an antenna dimer, we can invert Eq. (6) to get G_{bg}, given α and the simulated $\mathrm{LDOS}_{\mathrm{r,a}}$. To verify this procedure, we use the retrieved α and G_{bg} to predict total and absorptive antenna LDOS, given as

$$\mathrm{LDOS}_{\mathrm{tot,a}} = \mathrm{LDOS}_{\mathrm{r,a}}/A, \tag{7}$$

$$\mathrm{LDOS}_{\mathrm{abs,a}} = \mathrm{LDOS}_{\mathrm{tot,a}} - \mathrm{LDOS}_{\mathrm{r,a}}, \tag{8}$$

respectively, with $A = \sigma_{\mathrm{scat}}/\sigma_{\mathrm{ext}}$ the antenna albedo that we obtain from the antenna cross-sections given by the dipole model (lines in Fig. 2g of the main text). Fig. 2h in the main text compares the simulated LDOS data to these expressions, showing good agreement. Note that we could have also retrieved G_{bg} by inverting an expression for the *total* antenna LDOS, which is similar to the first term in Eq. (3) of the main paper. However, by using the radiative LDOS instead we are less sensitive to quenching and higher-order multipole resonances, which mainly affect $\mathrm{LDOS}_{\mathrm{abs,a}}$ and not $\mathrm{LDOS}_{\mathrm{r,a}}$.

With cavity and antenna parameters known, we can calculate LDOS spectra using Eq. (3) in the main paper. Moreover, for several figures in the main paper, including the various Q-$\tilde{V}$ diagrams, we determine hybrid Q and $\tilde{V}$. In that case, we use Eqs. (4-5) in the main text.

References

[1] Santhosh K, Bitton O, Chuntonov L, Haran G. Vacuum Rabi splitting in a plasmonic cavity at the single quantum emitter limit. Nat. Commun. 2016;7:11823.

[2] Doeleman HM, Verhagen E, Koenderink AF. Antenna-Cavity Hybrids: Matching Polar Opposites for Purcell Enhancements at Any Linewidth. ACS Photonics. 2016;3:1943–1951.

[3] De Vries, P, van Coevorden, DV, Lagendijk A. Point scatterers for classical waves. Rev. Mod. Phys. 1998; 70:447.

[4] Novotny L, Hecht B. Principles of nano-optics. 2nd ed. New York: Cambridge University Press; 2012.